Hindawi
International Journal of Aerospace Engineering
Volume 2020, Article ID 9587813, 11 pages
https://doi.org/10.1155/2020/9587813

Research Article

Comprehensive Performance Analysis for the Rotating Detonation-Based Turboshaft Engine

Zifei Ji,[1,2] Ruize Duan,[1] Renshuai Zhang,[1] Huiqiang Zhang,[1] and Bing Wang[1]

[1]*School of Aerospace Engineering, Tsinghua University, Beijing 100084, China*
[2]*Shenyang Engine Research Institute, Aero Engine Corporation of China, Shenyang 110015, China*

Correspondence should be addressed to Bing Wang; wbing@tsinghua.edu.cn

Received 13 January 2020; Revised 13 May 2020; Accepted 27 May 2020; Published 2 July 2020

Academic Editor: Wei Lin

The potential advantages of rotating detonation combustion are gradually approved, and it is becoming a stable and controllable energy conversion way adopted to the propulsion devices or ground-engines. This study focuses on the rotating detonation-based turboshaft engine, and the architecture is presented for this form of engine with compatibility between the turbomachinery and rotating detonation combustor being realized. The parametric performance simulation model for the rotating detonation-based turboshaft engine are developed. Further, the potential performance benefits as well as their generation mechanism are revealed, based on the comprehensive performance analysis of the rotating detonation-based turboshaft engine. Comparisons between the rotating detonation turboshaft engine and the conventional one reveal that the former holds significant improvements in specific power, thermal efficiency, and specific fuel consumption at lower compressor pressure ratios, and these improvements decrease with the increase of compressor pressure ratio and increase as turbine inlet temperature increases. The critical compressor pressure ratio corresponding to the disappearance of specific power improvement is higher than that corresponding to the disappearance of thermal efficiency and specific fuel consumption. These critical compressor pressure ratios are positively correlated with flight altitude and negatively correlated with flight velocity. The conductive research conclusion is guidable for the design and engineering application of rotating detonation-based engines.

1. Introduction

The helicopters have promising development and application foreground in both military and civil fields, owing to their superior performance operating at low altitude, low velocity, and maneuvering flight conditions. The turboshaft engine is the unique powerplant for the helicopter; therefore, advanced technologies for turboshaft engines have attracted significant interest in both academia and industry. The regenerative cycle and variable capacity technologies have the potential for improving the overall performance of the turboshaft engine, but the low technical maturity and poor technical versatility currently may be unacceptable. The turboshaft engine with simple cycle is still the first choice of advanced technology programs at present [1, 2].

For the conventional turboshaft with simple cycle, the key to enhancing the overall performance is to improve the total pressure ratio and temperature ratio [3]. After several decades of developments, the performance improvement of conventional turboshaft engine has entered a bottleneck period, as shown in Figure 1 [2]. Pressure-gain combustion is a prospective technology for the further performance improvement of the turboshaft with simple cycle [4]. Rotating detonation is a form of pressure-gain combustion, and it holds many potential advantages, such as high intensity of reaction, high thermal efficiency, and low entropy increase [5–7], which are helpful to improve the thrust and fuel consumption performance and reduce the structural weight. In the past decades, numerous studies relating to the ignition and detonation initiation performance, the operating diagram, and the unstable modes and their generation mechanism of the rotating detonation combustor (RDC) are experimentally performed, and the detailed flowfield structure and cellular structure information are revealed by multidimensional numerical methods [8–12]. The above studies have made the rotating detonation technology being

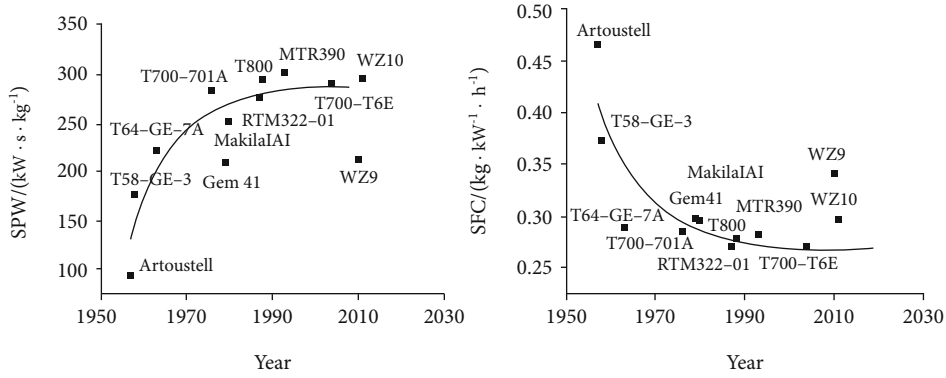

Figure 1: Technical trend of representative conventional turboshaft engines [2].

regarded as a stable and controllable energy conversion way. Naples et al. [13, 14] studied the interaction between the RDC and conventional turbine elements by the integration system of the T63 turboshaft engine embedded with an RDC. With the main combustor of GTD-350 engine being replace by an RDC, the feasibility of the RDC being applied to turboshaft engine has been confirmed by Wolański [15]. George et al. [16, 17] experimentally investigated the axial turbine performance operating under pulsating flows, which hold the similar features with the detonation chamber exhaust, and approved that the pressure oscillations may lead to undesirable turbine performance degradation. With the performance of the supersonic turbine being characterized by the power extraction and total pressure loss parameters, Liu et al. [18, 19] numerically studied the effects of unsteady inlet conditions on the operating characteristics of the supersonic turbine and revealed that leading edge shock waves were the main factor for the unsteady loss mechanism. Sousa et al. [20] analyzed the thermodynamic performance of the gas turbine with an RDC with the T-MATS software coupled with the MOC solver of RDC model; the result showed that the thermal efficiency of the rotating detonation turbine engine could be 5% higher than that of the conventional one at low compressor pressure ratios, but the performance benefits decreased as the compressor pressure ratio increased. With the accumulation of the achievements on rotating detonation turbine engine, the feasibility and potential advantages of this new form of engine are gradually approved [20–23]. However, studies regarding the overall performance characteristics and the potential performance benefits as well as their generation mechanism of the turboshaft engine embedded with an RDC are quite scarce. Compared to the conventional turboshaft engine, the study of rotating detonation-based turboshaft engine is still in its infancy.

This study aims at revealing the potential performance benefits of the rotating detonation-based turboshaft engine and promoting further application of RDC in propulsion systems. Firstly, the parametric cycle analysis model of the rotating detonation-based turboshaft engine is developed based on the low-order analytical model of RDC and the compatibility relationship between the turbomachinery and RDC. Then, the overall performance characteristics of the new form of engine are achieved. Finally, a performance comparison between the rotating detonation-based turboshaft engine and the conventional one is performed, and the performance benefits as well as their generation mechanism are revealed.

2. Mathematical and Physical Model

2.1. System Formulation. With the compatibility between RDC and turbomachinery under consideration, the isolator and mixer chamber are arranged upstream and downstream from RDC, respectively, in the dual-duct rotating detonation aeroturbine engine (DRDATE) [22]. With the power turbine and power shaft arranged downstream from the turbine of the DRDATE (which is used as the gas generator), a configuration for the rotating detonation-based turboshaft engine is proposed, as shown in Figure 2(a). Figure 2(b) further displays the ideal thermodynamic cycle process comparison between the rotating detonation-based turboshaft engine and the conventional one. For the rotating detonation-based turboshaft engine, air flows into the engine at state 0; the process 0-3 is the integrated compression process proceeding in the intake, isolator, and compressor; the processes $3'$-$3.5'$ and $3.5'$-$4'$ represent the shock compression and heat release due to combustion, respectively; the process $4'$-$9'$ represents the integrated expansion process proceeding in the turbine, power turbine, and nozzle; and the thermodynamic cycle is closed via the imaginary exothermic process $9'$-0. The thermodynamic cycle processes of the conventional turboshaft engine can be analyzed in exactly the same manner.

The final temperature of the heating process in rotating detonation-based turboshaft engine is higher than that in the conventional turboshaft engine with the same heat addition, as the specific heat capacity of detonation process is lower than that of the deflagration process. Therefore, the former corresponds less entropy production, which implies the heat loss owing to exhaust (which can be estimated with the projected area of the exothermic process to *s*-axis, as shown in Figure 2(b)) of the rotating detonation-based turboshaft engine is higher than that of the conventional one. The above has revealed the thermal efficiency benefit of the rotating detonation turbine engine conceptually.

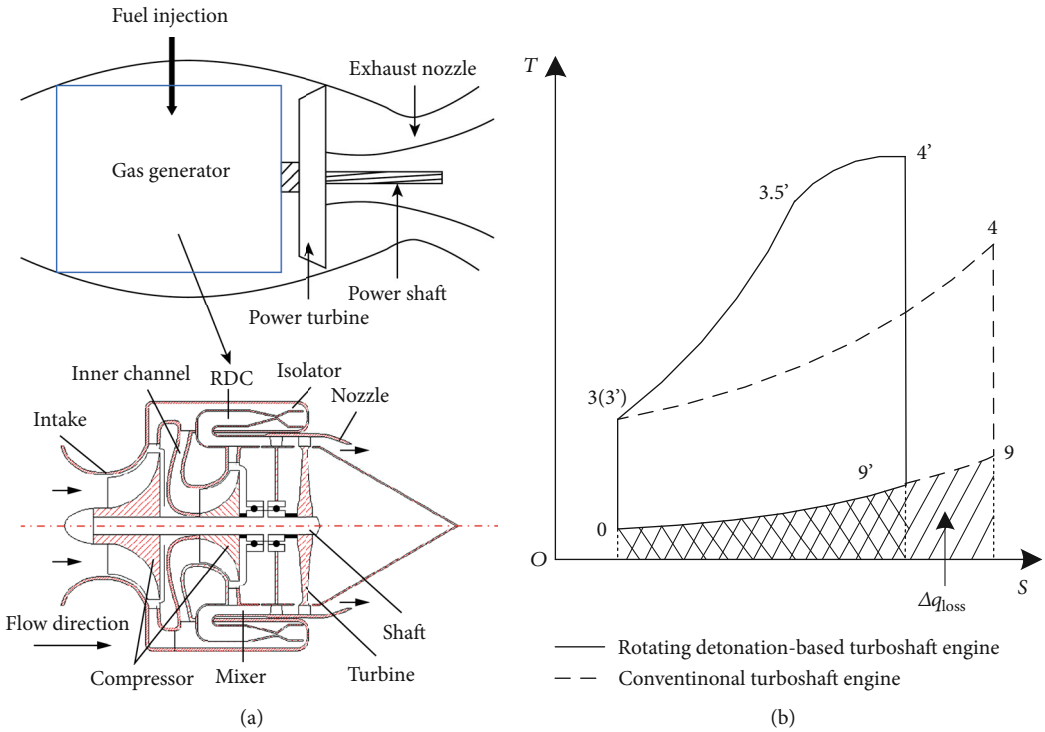

Figure 2: (a) Configuration and (b) ideal thermodynamic cycle processes of the rotating detonation-based turboshaft engine.

2.2. Parametric Cycle Analysis Model. The thermodynamic processes proceeding in the rotating detonation-based turboshaft engine can be simplified as "polytropic compression-rotating detonation-adiabatic mixing-polytropic expansion," and the reduced order model which was developed based on the matching relationship between the injection process and pressure decay after the detonation front [22] is adopted in this study for the estimation of the rotating detonation process. The RDC is fueled by kerosene, and the reaction mechanism is taken from [24]. The models of the remaining processes are consistent with the conventional turboshaft engine. The thermodynamic process in the conventional compressor can be regarded as nonisentropic polytropic compression, and the mathematical model can be expressed as follows:

$$p_3^* = \pi_c p_1^*, \tag{1}$$

$$\int_{T_1^*}^{T_3^*} c_p \frac{dT}{T} = R_0 \ln \pi_c, \tag{2}$$

$$h_3^* = h_1^* + \int_{T_1^*}^{T_3^*} c_p dT, \tag{3}$$

$$\eta_c = \frac{h_{3i}^* - h_1^*}{h_3^* - h_1^*}. \tag{4}$$

where h_{3i}^* is the total enthalpy corresponding to the isentropic compression with a compression pressure ratio π_c. The thermodynamic process in the turbine can be modeled in exactly the same way.

The gas properties are a function of the gas temperature. In this study, the parametric performance simulation model of the engine is developed based on the "variable-γ" strategy. Firstly, the gas properties of the single component can be calculated by polynomial fitting of temperature (the polynomial coefficients are referred to NASA [25]); then, the gas properties of working medium can be obtained by mass flow average.

$$c_{pi} = R_i\left(a_{0i} + a_{1i}T + a_{2i}T^2 + a_{3i}T^3 + a_{4i}T^4\right), \tag{5}$$

$$c_p = \sum_{i=1}^{N} c_{pi} Y_i, \tag{6}$$

$$\gamma = \frac{\sum_{i=1}^{N} c_{pi} Y_i}{\sum_{i=1}^{N} Y_i \left(c_{pi}/\gamma_i\right)}. \tag{7}$$

Similar to the conventional turboshaft engine, specific power P_s, thermal efficiency η_{th}, and specific fuel consumption sfc are used as metrics to characterize the overall performance of the rotating detonation-based turboshaft engine. According to the parametric cycle analysis model and component matching equations, the performance metrics can be calculated by Equations (4)–(6). And α represents the air split parameter, which is the ratio of the mass flow rate of the inner duct to that of the outer duct in DRDATE. κ is the power split parameter, which is adopted to characterized the power split between the power turbine and the nozzle. According to the representative turboshaft engines, the value of κ is taken as 0.96.

Table 1: Uncertainty analysis of the performance metrics of the rotating detonation-based turboshaft engine.

Performance metrics	P_s		η_{th}		sfc	
Cycle parameters	p_4^*	T_4^*	p_4^*	T_4^*	p_4^*	T_4^*
ε	10%	10%	10%	10%	10%	10%
u_i $(i = 1, 2)$	0.96%	3.31%	2.14%	9.39%	2.09%	9.37%
u	4.19%		9.63%		9.60%	

The subscripts 6 and 9 represent the parameters of power turbine inlet and exhaust nozzle outlet sections, respectively.

$$P_s = \left(1 + \frac{f}{1+\alpha}\right)\kappa h_6^* \left[1 - \left(\frac{p_9}{p_6^*}\right)^{(\gamma-1)/\gamma}\right], \tag{8}$$

$$\eta_{th} = P_s/[f \cdot H_f/(1+\alpha)], \tag{9}$$

$$sfc = 3600f/[P_s(1+\alpha)]. \tag{10}$$

The utilization of reduced order model of RDC can introduce calculation errors, owing to the assumptions. Compared to the 2D CFD solver, the calculation error of the reduced order model is below 10% [22, 23]. The overall uncertainty of the performance metrics of the rotating detonation-based turboshaft engine can be estimated by the sensitivity analysis of the calculation errors of RDC outlet parameters on overall performance of the engine. Assuming that Ψ is the performance metric; then, the overall uncertainty of Ψ can be calculated by

$$u_1 = [\Psi(p_4^* + \varepsilon p_4^*) - \Psi(p_4^*)]/\Psi(p_4^*), \tag{11}$$

$$u_2 = [\Psi(T_4^* + \varepsilon T_4^*) - \Psi(T_4^*)]/\Psi(T_4^*), \tag{12}$$

$$u = \sqrt{\sum u_i^2} = \sqrt{u_1^2 + u_2^2}, \tag{13}$$

where ε is the model error of RDC, u_i represents the uncertainty component, and u represents the overall uncertainty. Table 1 summarizes the uncertainty components and overall uncertainty of the P_s, η_{th}, and sfc, which are generated by the calculation errors of the RDC model. It shows that the overall uncertainties of performance metrics remain at a relatively low level (<10%). In addition, the uncertainty of P_s is lower than that of η_{th} and sfc.

3. Results and Discussions

3.1. Sensitivity Analysis of Component Parameters on Overall Performance of the Engine. A sensitivity analysis is conducted below to reveal the variation in overall performance of the rotating detonation-based turboshaft engine versus the component parameters. The compressor pressure ratio π_c and turbine inlet temperature T_4^* play a major role in the overall performance of the engine. The variations in P_s, η_{th}, and sfc with respect to π_c and T_4^* under standard sea-level and high altitude cruise conditions are, respectively, illustrated in Figures 3 and 4. In the figures, the coordinate values of each points are determined by the P_s and sfc of the cases with the corresponding values of π_c and T_4^*, and the values of η_{th} are presented by the color scales. The sensitivity of performance metrics to the π_c and T_4^* can be presented intuitively by the trends of curves and color scales. It can be seen that, with an increase in π_c, P_s and η_{th} first increase but then decrease, and sfc first decreases but then increases. As π_c increases, on the one hand, the power turbine pressure ratio π_t increases, and the sensitivity of π_t to changes in π_c decreases, as the pressure-gain of the RDC is negatively correlated with π_c [22]. On the other hand, the cycle heat addition decreases owing to the increase of combustor inlet temperature T_3^* and air split parameter α. In addition, the increase of α can weaken the potential benefits relating to the pressure gain of the RDC. At low values of π_c, the increase of π_t is the main factor influencing P_s, and P_s increases with the increase of π_c. As π_c increases, the increase of T_3^* and α becomes the dominant factor influencing P_s, and P_s decreases as π_c increases. The thermal efficiency η_{th} is positively correlated with P_s, so the variation of η_{th} is consistent with that of P_s. In addition, η_{th} is positively correlated with α according to Equation (9), so the unfavorable impact of T_3^* can be weakened. Therefore, the downward trend of η_{th} at high values of π_c is less obvious than that of P_s. On the basis of Equation (10), sfc is actually determined by P_s, α, and fuel-air ratio f. When T_4^* remains constant, α is positively correlated with π_c, and f is negatively correlated with π_c. At low values of π_c, the increase of P_s and α and the decrease of f are all favorable factors for reducing sfc. When the value of π_c is relatively high, the favorable effects due to the increase of α and decrease of f are not sufficient to overcome the effect unfavorable effect from the decrease in P_s, and the variation of sfc shows opposing trend. As shown in Figures 3 and 4, the isopleths of η_{th} run nearly parallel to the horizontal ordinate, which implies that there is a strong correction between the variation of η_{th} and that of sfc.

When the compressor pressure ratio π_c remains constant, P_s and η_{th} exhibit positive correlation with T_4^*, and sfc exhibits negative correlation with T_4^*. Furthermore, the performance metrics are less sensitive to changes in T_4^* than them to changes in π_c. As T_4^* increases, the cycle heat addition increases, resulting in the proportion of heat loss owing to exhaust decreases, which is favorable for the improvement of η_{th}. In addition, η_{th} is positively correlated with α, and α decreases with the increase of T_4^*. Therefore, the improvement of η_{th} due to the increase of cycle heat addition is weakened by the effect of α. In summary, η_{th} increases with an increase in T_4^*, and the sensitivity of η_{th} to changes in T_4^* decreases with an increase in T_4^*. The variation sfc can be explained in exactly the same manner. For a constant value

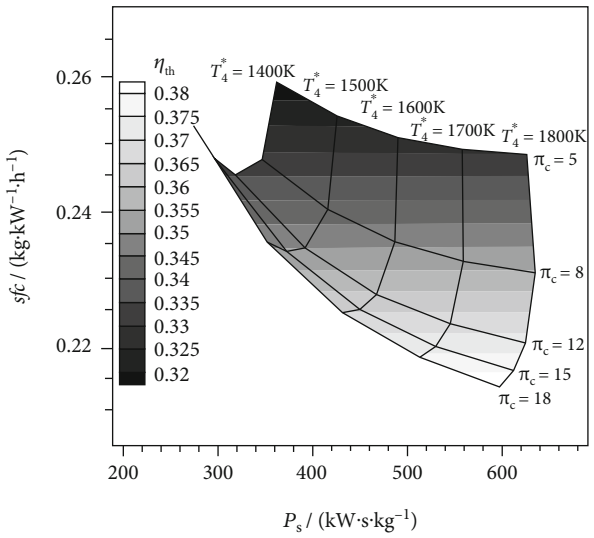

Figure 3: Variations in performance metrics with cycle parameters under standard sea-level condition.

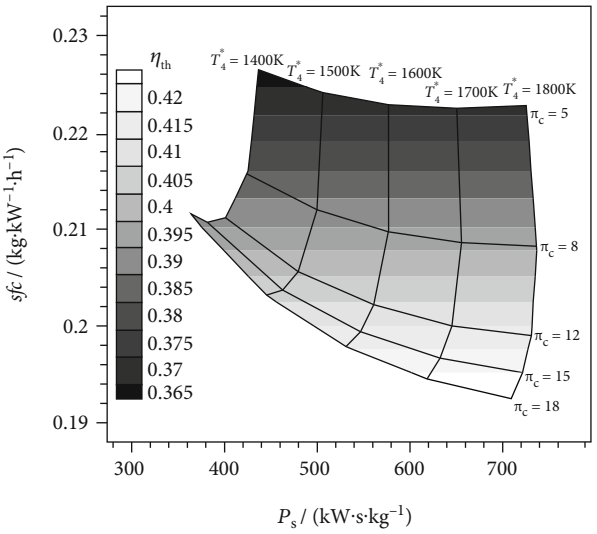

Figure 4: Variations in performance metrics with cycle parameters under high altitude cruise condition.

of π_c, P_s is actually determined by the cycle heat addition. Therefore, P_s increases monotonically with the increase of $T_4{}^*$. Generally, the application of rotating detonation technology does not change the variation trends of performance metrics of the turboshaft engine versus cycle parameters.

There is strong agreement between the variation trends of performance metrics under high-altitude cruise condition and those under standard sea-level condition versus cycle parameters. Under cruise condition, the total pressure ratio improves owing to the ram compression, and so do the performance metrics. As H increases, the freestream temperature T_0 as well as the combustor inlet temperature $T_3{}^*$ decreases, which is favorable for the total pressure gain in the RDC. Therefore, the high-altitude cruise condition corresponds to higher P_s and η_{th} and lower sfc.

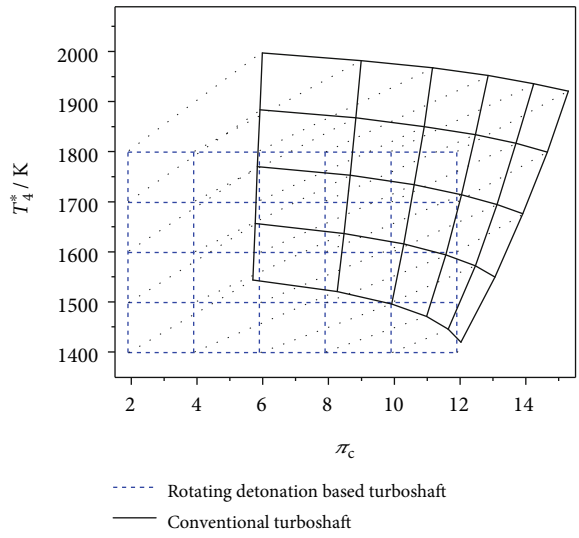

Figure 5: Cycle parameters mapping between the rotating detonation turboshaft engine and the conventional one with the same performance metrics.

The cycle parameter comparison between the rotating detonation-based turboshaft engine and the conventional one with the same performance metrics is displayed in Figure 5. It can be seen that the former corresponds to a lower π_c and $T_4{}^*$. The reduction in π_c is conducive to improving the structural compactness and power weight ratio, and the reduction in $T_4{}^*$ is a benefit for increasing the service life of the turbine. Furthermore, the benefits of reducing π_c and $T_4{}^*$ exhibit a positive correlation with $T_4{}^*$ and a negative correlation with π_c, and the internal mechanism is consistent with the variations in performance benefits versus π_c and $T_4{}^*$, which have been expressed above.

The feedback pressure perturbation generated by the RDC can be reduced effectively by the isolator, but it cannot be eliminated thoroughly [22]. The weakened pressure perturbation may result in reduction in compressor efficiency. Similarly, the turbine inlet parameter distribution can be improved owing to the mixing process in the mixer, but the turbine inlet parameter distribution of the rotating detonation-based turboshaft engine, which has a direct relationship with the turbine efficiency, is still less uniform than that of the conventional one. Therefore, the sensitivity analysis of turbomachinery efficiency and the total pressure recovery of the isolator on overall performance of the rotating detonation-based turboshaft engine is of significance. As the turbomachinery polytropic efficiency e_c and e_t is hardly dependent on the pressure ratios π_c and π_t [3], e_c and e_t are utilized to characterize the turbomachinery efficiency in this study. Figure 6 displays the effects of compressor polytropic efficiency e_c, turbine polytropic efficiency e_t and total pressure recovery coefficient of isolator σ_{is} on the overall performance of the engine. As π_c remains constant, the increase of e_c and e_t could improve the overall performance of the engine. And the performance metrics are more sensitive to changes in e_c and e_t at higher values of π_c. Furthermore, P_s and sfc are more sensitive to changes in e_c than to changes

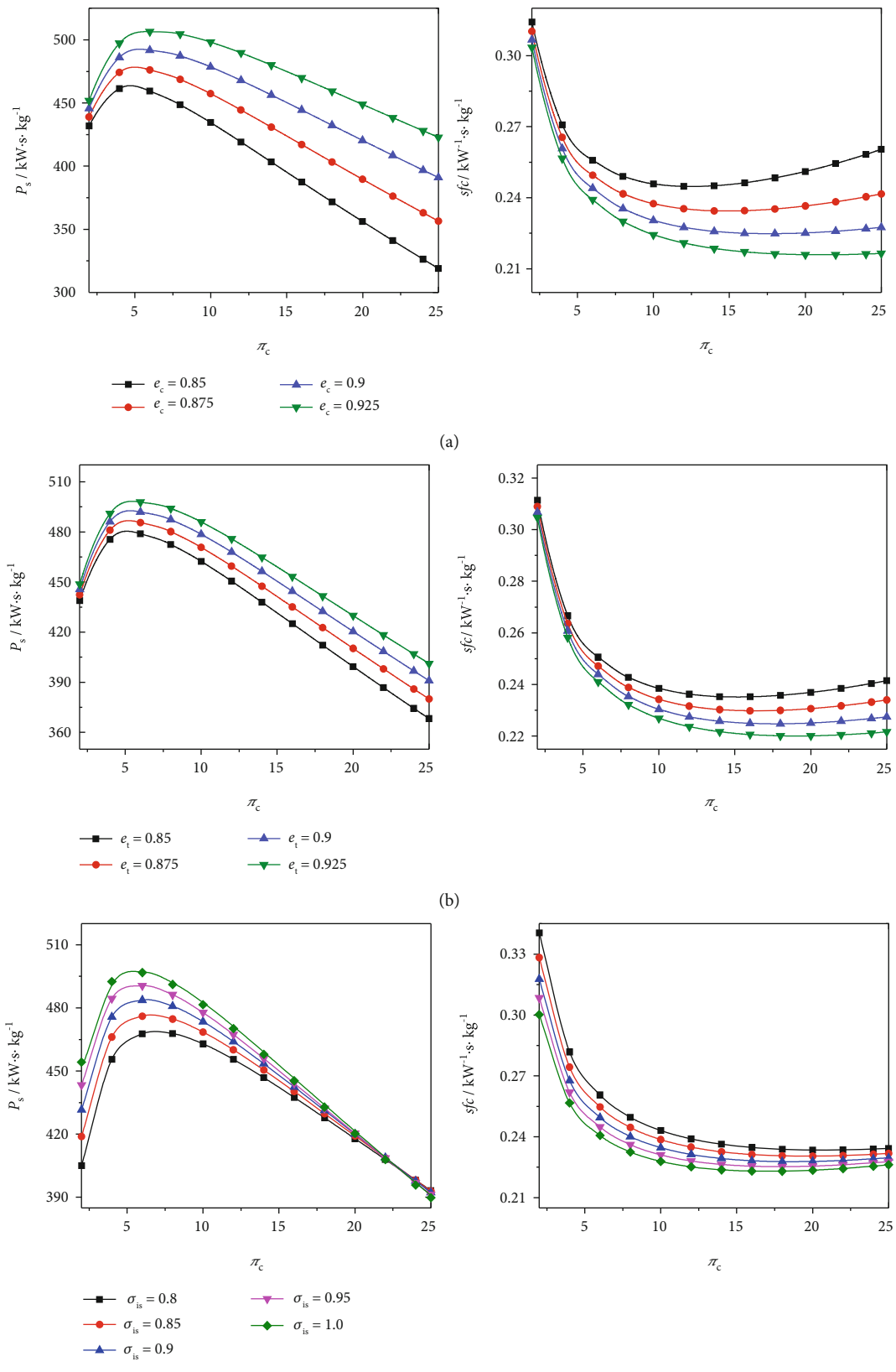

Figure 6: Variations in performance metrics with (a) compressor polytropic efficiency e_c, (b) turbine polytropic efficiency e_t, and (c) total pressure recovery coefficient of isolator σ_{is}.

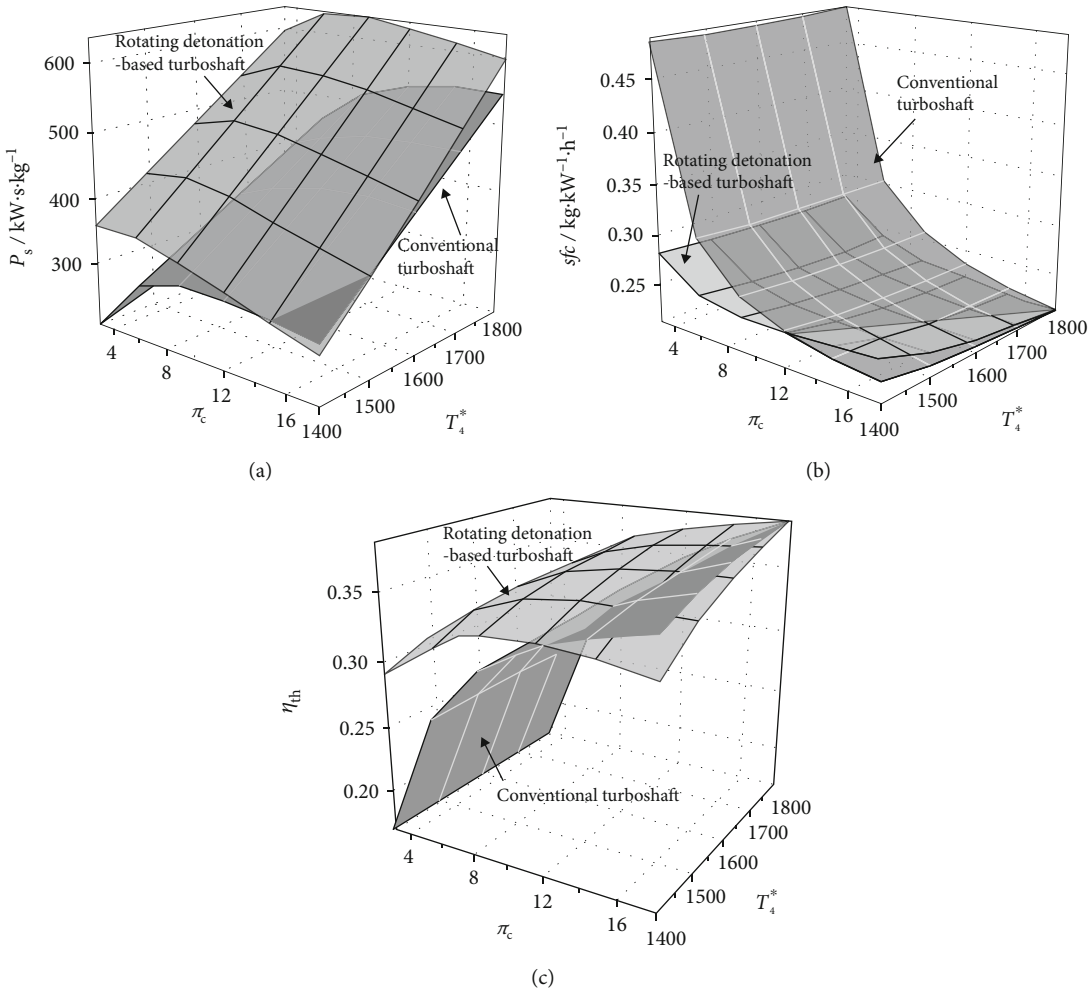

Figure 7: Performance comparison of turboshaft engine based on rotating detonation and the conventional one for different cycle parameters. (a) P_s, (b) sfc, and (c) η_{th}.

in e_t, as the compressor pressure ratio is normally higher than the turbine pressure ratio. Unlike the influence mechanism of e_c and e_t, the increase of σ_{is} has the same impact as improving the total pressure ratio of the engine. According to the sensitivity analysis of cycle parameters on overall performance of the engine, as π_c increases, P_s first increases but then decreases, and sfc first decreases but then increases. At low values of π_c, the higher the value of σ_{is}, the higher the value of P_s. When the value of π_c is relatively high, the situation is the opposite. As the optimum compressor pressure ratios corresponding to the maximum η_{th} and minimum sfc are higher than that corresponding to the maximum P_s, when the values of π_c are not quite high, the higher the value of σ_{is}, the higher the value of η_{th} and the lower the value of sfc.

3.2. Comparison Between the Rotating Detonation-Based Turboshaft Engine and the Conventional One. Figure 7 shows the variations in performance difference between the rotating detonation-based turboshaft engine and the conventional one with the same component parameters versus cycle parameters under the standard sea-level condition at take-off. It can be seen that, at low values of π_c, the rotating detonation-based turboshaft engine exhibits significant potential benefits in P_s, η_{th}, and sfc. As π_c increases, the potential benefits decrease and tend to disappear. Furthermore, the compressor pressure ratio range corresponding to the rotating detonation-based turboshaft engine exhibiting benefit in P_s is wider than that corresponding to the engine exhibiting benefit in η_{th} and sfc. The fuel-air ratio f of the rotating detonation-based turboshaft engine is higher than that of the conventional one with the same cycle parameters. Then, the total pressure gain of the RDC is significant at low values of π_c, resulting in a higher power turbine pressure ratio π_{pt} of the rotating detonation-based turboshaft engine compared to the conventional one. As the total pressure gain of the RDC decreases with an increase in π_c, so does the benefit of π_{pt}. For the η_{th} and sfc of turboshaft engines, the higher value of f is an unfavorable factor, and the higher value of π_{pt} is a favorable factor. The potential benefits of η_{th} and sfc can be achieved by the rotating detonation-based turboshaft engine under the premise that the favorable effects generated by π_{pt} are sufficient to overcome the unfavorable effects of a higher value of f. Therefore, there is a strong agreement between the variations of the potential benefits in η_{th} and sfc and the variation of

the benefit of π_{pt}. The higher value of f and the higher value of π_{pt} are all favorable factors for the improvement of P_s. Therefore, the rotating detonation-based turboshaft engine exhibits significant benefit in P_s at low values of π_c. In addition, the power turbine inlet total enthalpy h_6^* of the rotating detonation-based turboshaft engine is lower than that of the conventional one, owing to the rear stage of compressor. Therefore, the benefit in P_s tends to disappear at high values of π_c. It is not difficult to draw the conclusion that the critical compressor pressure ratio π_{crit1} corresponding to the disappearance of P_s improvement is higher than that corresponding to the disappearance of η_{th} and sfc, according to the above explanation.

When the value of π_c remains constant, as T_4^* increases, the potential performance benefits of the rotating detonation-based turboshaft engine increase continuously. And the potential benefits in η_{th} and sfc are more sensitive to changes in T_4^* compared to the potential benefit in P_s. Although the total pressure gain of the RDC is independent of T_4^*, the effect of the total pressure gain of the RDC can be enlarged owing to the decrease of α. Therefore, the performance differences between the rotating detonation-based turboshaft engine and the conventional one increase with an increase in T_4^*. In addition, the fuel-air ratio difference increases as T_4^* increases owing to the decrease of α. As η_{th} is positively correlated with P_s and negatively correlated with f, the potential benefits in η_{th} is more sensitive to changes in T_4^*. According to the explanation in Section 3.1, there is a strong correction between the variation of η_{th} and that of sfc, so do the variations of performance benefits in η_{th} and sfc. The variations in critical compressor pressure ratio π_{crit1} corresponding to the disappearance of P_s improvement and the critical compressor pressure ratio π_{crit2} corresponding to the disappearance of sfc improvement of the rotating detonation-based turboshaft engine versus T_4^* are displayed in Table 2. It can be seen that π_{crit1} and π_{crit2} exhibit positive correlation with T_4^*, and π_{crit1} is normally larger than π_{crit2}.

As the value of π_c remains constant at 12 and the value of T_4^* remains constant at 1600 K, the variations in performance differences between the rotating detonation-based turboshaft engine and the conventional one versus flight parameters are shown in Figure 8. As V_0 increases, P_s and η_{th} of the two forms of engines increase, and sfc decreases monotonically. And the performance differences between the two forms of engines decreases with an increase in V_0. And the performance differences of η_{th} and sfc are more sensitive to changes in V_0 compared to the performance difference of P_s. As V_0 increases, the total pressure ratio of the engine increases owing to the ram compression, which is favorable for improving the overall performance. The performance benefits of the rotating detonation-based turboshaft engine compared to the conventional one are mainly contributed by the total pressure gain of the RDC. As V_0 increases, the combustor inlet temperature T_3^* increases, which is detrimental to the total pressure gain of the RDC [22, 23]. In addition, α increases with an increase in V_0, owing to the decrease of cooling capacity of the compressed air. Then, the effect of the total pressure gain of the RDC can be weakened. In summary, the potential performance benefits of the rotating detonation-based turboshaft decrease with an increase in V_0. P_s and η_{th} of the two forms of engines exhibit a positive correlation with H, and sfc exhibits a negative correlation with H. And the performance differences between the two forms of engines exhibit a positive correction with H. With the increase of H, the freestream temperature T_0 decreases monotonically, which is favorable for the improvement of the overall performance. T_3^* decreases with an increase in H, resulting in the improvement of the total pressure gain of the RDC. In addition, α decreases with an increase in H, and the effect of the total pressure gain of the RDC can be enlarged. With the combined effects of these two factors, the potential performance benefits of the rotating detonation-based turboshaft increase with an increase in H. The effects of flight parameters on π_{crit1} and π_{crit2} are displayed in Tables 3 and 4. According to the calculation results, π_{crit1} and π_{crit2} are positively correlated with H and negatively correlated with V_0.

Table 2: Variations in critical compressor pressure ratios π_{crit1} and π_{crit2} with T_4^*.

T_4^*, K	π_{crit1}	π_{crit2}
1400	14.20	12.37
1500	18.23	13.87
1600	23.52	15.26
1700	30.69	16.5
1800	40.87	17.71

3.3. Optimum Pressure Ratios. On the basis of the variations in P_s and sfc of the rotating detonation-based turboshaft engine versus π_c, there exist an optimum compressor pressure ratio π_{opt1} that maximizes the specific power and an optimum compressor pressure ratio π_{opt2} that minimizes the specific fuel consumption. Table 5 shows the variations in π_{opt1} and π_{opt2} versus T_4^*. It can be seen that π_{opt1} and π_{opt2} increase with an increase in T_4^*, as P_s exhibits a positive correlation with T_4^* and sfc exhibits a negative correlation with T_4^*. The variations in π_{opt1} and π_{opt2} versus flight parameters V_0 and H are listed in Tables 6 and 7. With the increase of V_0, the optimum compressor pressure ratios decrease continuously owing to the ram compression. As H increases, the RDC inlet temperature decreases, and the pressure gain of the RDC increases monotonically. In addition, α decreases as the freestream temperature decreases with an increase in H. For the effects of the above factors, sfc performance improves with H as does π_{opt2}.

4. Conclusion

In this study, a configuration of the rotating detonation-based turboshaft engine with the compatibility between the turbomachinery and RDC under consideration is presented. Then, the performance characteristics of this new form of engine are investigated based on the parametric

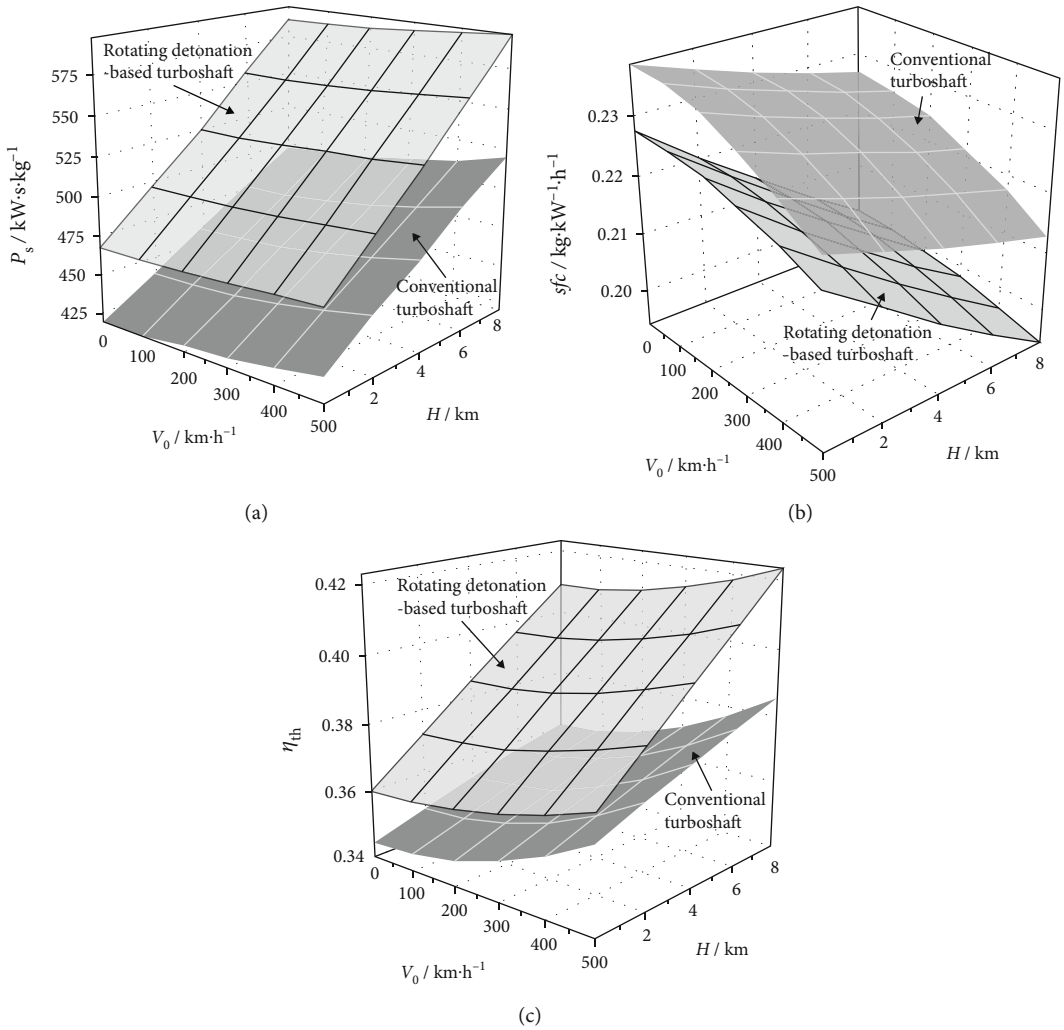

Figure 8: Performance comparison of turboshaft engine based on rotating detonation and the conventional one for different cycle parameters. (a) P_s, (b) sfc, and (c) η_{th}.

Table 3: Variations in critical compressor pressure ratios π_{crit1} and π_{crit2} with V_0.

V_0, km h^{-1}	π_{crit1}	π_{crit2}
0	23.52	15.26
150	23.32	15.1
300	22.72	14.63
450	21.77	13.89

Table 4: Variations in critical compressor pressure ratios π_{crit1} and π_{crit2} with H.

H, km	π_{crit1}	π_{crit2}
0	21.77	13.89
2	23.72	15.4
4	25.94	17.17
6	28.45	19.27
8	31.35	21.77

Table 5: Variations in optimum compressor pressure ratios π_{opt1} and π_{opt2} with $T_4{}^*$.

$T_4{}^*$, K	π_{opt1}	π_{opt2}
1400	4.18	11.04
1500	4.95	14.07
1600	5.79	17.67
1700	6.68	21.93
1800	7.71	26.52

Table 6: Variations in optimum compressor pressure ratios π_{opt1} and π_{opt2} with V_0.

V_0, km h^{-1}	π_{opt1}	π_{opt2}
0	5.79	17.67
150	5.73	17.56
300	5.55	17.28
450	5.31	16.81

Table 7: Variations in optimum compressor pressure ratios π_{opt1} and π_{opt2} with H.

H, km	π_{opt1}	π_{opt2}
0	5.40	16.98
2	5.66	18.73
4	5.94	20.76
6	6.25	23.13
8	6.60	25.92

thermodynamic cycle analysis model. In order to reveal the potential performance benefits and their generation mechanism, the performance comparison between the rotating detonation-based turboshaft engine and the conventional one is performed. The major conclusions are summarized as follows.

(1) When the flight parameters remain constant, as the compression ratio π_c increases, the specific power P_s and thermal efficiency η_{th} of the rotating detonation-based turboshaft engine first increase but then decrease, and the specific fuel consumption sfc first decreases but then increases. As the turbine inlet temperature T_4^* increases, P_s and η_{th} increase, and sfc decreases continuously. When the component parameters remain constant, with the increase in flight velocity V_0 and flight altitude H, P_s and η_{th} increase, and sfc decreases monotonically. There exist optimum compressor pressure ratios π_{opt1} and π_{opt2} which maximizes the specific power and minimizes the specific fuel consumption, respectively, and π_{opt1} is nominally larger than π_{opt2}. Furthermore, π_{opt1} and π_{opt2} are positively correlated with T_4^* and H and are negatively correlated with V_0.

(2) Compared to the conventional turboshaft engine, the thermal efficiency of the rotating detonation-based turboshaft engine can be improved above 7% at lower values of π_c, and the benefits decrease with an increase in π_c. As π_c remains constant, the performance improvements increase with the increase of T_4^*. As T_4^* remains constant at 1600 K, the value of π_{crit1} is about 23.5 corresponding to the disappearing of benefit in P_s, and value of π_{crit2} is about 15.3 corresponding to the disappearing of benefit in η_{th} and sfc. The critical compressor pressure ratios are positively correlated with T_4^* corresponding to the disappearance of performance benefits.

(3) When the value of π_c is not quite high and the value of T_4^* is not relatively low, the rotating detonation-based turboshaft engine exhibits competitive potential benefits within the typical flight envelope of helicopters (i.e., $V_0 < 450$ km/h and $H < 8$ km). The potential benefits of the rotating detonation-based turboshaft engine exhibit a positive correlation with H and exhibit a negative correlation with V_0. Furthermore, the values of π_{crit1} and π_{crit2} increase with the increase in H and decrease with an increase in V_0.

Nomenclature

c_p: Specific heat at constant pressure
f: Fuel-air mass flow ratio
H_f: Fuel heating value
h: Enthalpy
Ma: Mach number
$\dot{m}$: Mass flow rate
P_s: Specific power
p: Pressure
R: Universal gas constant
sfc: Specific fuel consumption
T: Temperature
u: Overall uncertainty
V: Velocity
γ: Ratio of specific heats
η_0: Overall efficiency
η_{th}: Thermal efficiency
κ: Power split parameter
π_c: Compressor pressure ratio.

Superscripts

*: Total or stagnation parameters.

Subscripts

0: Freestream at the intake entrance
1: Compressor inlet section
3: Combustor inlet section
4: Turbine inlet section
6: Power turbine inlet section
9: Nozzle outlet section.

Abbreviations

DRDATE: Dual-duct rotating detonation aeroturbine engine
RDC: Rotating detonation combustor.

Data Availability

The data used to support the findings of this study are available from the corresponding author upon request.

Conflicts of Interest

The authors declare that there is no conflict of interest regarding the publication of this paper.

Acknowledgments

This work is supported in part by the National Natural Science Foundation of China (No. 51676111) and Science and Technology on Liquid Rocket Engine Laboratory Fund (No. 61427040102).

References

[1] E. T. Johnson and H. Lindsay, "Advanced technology programs for small turboshaft engines: past, present, future," *Journal of Engineering for Gas Turbines and Power*, vol. 113, no. 1, pp. 33–39, 1991.

[2] N. Ge, "Development and technical trend of turbo shafts engine," *Journal of Nanjing University of Aeronautics & Astronautics*, vol. 50, no. 2, pp. 145–156, 2018.

[3] S. Farokhi, *Aircraft Propulsion*, John Wiley & Sons, New York, NY, USA, 2nd edition, 2014.

[4] G. A. Richards, *New Developments in Combustion Technology - Part II: Step Change in Efficiency*, Princeton-CEFRC Summer School on Combustion, Princeton, NJ, US, 2012.

[5] F. A. Bykovskii, S. A. Zhdan, and E. F. Vedernikov, "Continuous spin detonations," *Journal of Propulsion and Power*, vol. 22, no. 6, pp. 1204–1216, 2006.

[6] P. Wolański, "Detonative propulsion," *Proceedings of the Combustion Institute*, vol. 34, no. 1, pp. 125–158, 2013.

[7] F. K. Lu and E. M. Braun, "Rotating detonation wave propulsion: experimental challenges, modeling, and engine concepts," *Journal of Propulsion and Power*, vol. 30, no. 5, pp. 1125–1142, 2014.

[8] J. Kindracki, P. Wolański, and Z. Gut, "Experimental research on the rotating detonation in gaseous fuels–oxygen mixtures," *Shock Waves*, vol. 21, no. 2, pp. 75–84, 2011.

[9] V. Anand and E. Gutmark, "Rotating detonation combustors and their similarities to rocket instabilities," *Progress in Energy and Combustion Science*, vol. 73, pp. 182–234, 2019.

[10] B. A. Rankin, D. R. Richardson, A. W. Caswell, A. G. Naples, J. L. Hoke, and F. R. Schauer, "Chemiluminescence imaging of an optically accessible non-premixed rotating detonation engine," *Combustion and Flame*, vol. 176, pp. 12–22, 2017.

[11] D. Schwer and K. Kailasanath, "Fluid dynamics of rotating detonation engines with hydrogen and hydrocarbon fuels," *Proceedings of the Combustion Institute*, vol. 34, no. 2, pp. 1991–1998, 2013.

[12] N. Tsuboi, S. Eto, A. K. Hayashi, and T. Kojima, "Front cellular structure and thrust performance on hydrogen-oxygen rotating detonation engine," *Journal of Propulsion and Power*, vol. 33, no. 1, pp. 100–111, 2017.

[13] A. Naples, J. Hoke, R. T. Battelle, M. Wagner, and F. R. Schauer, *Rotating Detonation Engine Implementation into an Open-Loop T63 Gas Turbine Engine*, AIAA Paper, 2017.

[14] A. Naples, J. Hoke, R. Battelle, and F. Schauer, "T63 turbine response to rotating detonation combustor exhaust flow," *Journal of Engineering for Gas Turbines and Power*, vol. 141, no. 2, article 021029, 2019.

[15] P. Wolański, "Application of the continuous rotating detonation to gas turbine," *Applied Mechanics and Materials*, vol. 782, pp. 3–12, 2015.

[16] A. S. George, R. B. Driscoll, D. E. Munday, and E. J. Gutmark, "Experimental comparison of axial turbine performance under pulsed air and pulsed detonation flows," AIAA Paper, 2013.

[17] A. S. George, R. Driscoll, E. Gutmark, and D. Munday, "Experimental comparison of axial turbine performance under steady and pulsating flows," *Journal of Turbomachinery*, vol. 136, no. 11, article 111005, 2014.

[18] Z. Liu, J. Braun, and G. Paniagua, *Three dimensional optimization for subsonic axial turbines operating at high unsteady inlet Mach number*, AIAA Paper, 2018.

[19] Z. Liu, J. Braun, and G. Paniagua, "Characterization of a supersonic turbine downstream of a rotating detonation combustor," *Journal of Engineering for Gas Turbines and Power*, vol. 141, no. 3, article 031501, 2019.

[20] J. Sousa, G. Paniagua, and E. C. Morata, "Thermodynamic analysis of a gas turbine engine with a rotating detonation combustor," *Applied Energy*, vol. 195, pp. 247–256, 2017.

[21] Z. Ji, H. Zhang, Q. Xie, and B. Wang, "Thermodynamic process and performance analysis of the continuous rotating detonation turbine engine," *Journal of Tsinghua University (Science and Technology)*, vol. 58, no. 10, pp. 899–905, 2018.

[22] Z. Ji, H. Zhang, and B. Wang, "Performance analysis of dual-duct rotating detonation aero-turbine engine," *Aerospace Science and Technology*, vol. 92, pp. 806–819, 2019.

[23] Z. Ji, H. Zhang, B. Wang, and W. He, "Comprehensive performance analysis of the turbofan with a multi-annular rotating detonation duct burner," *Journal of Engineering for Gas Turbines and Power*, vol. 142, no. 2, 2020.

[24] F. Ladeinde, X. Cai, B. Sekar, and B. Kiel, *Application of combined LES and flamelet modeling to methane, propane, and Jet-A combustion*, AIAA Paper, 2001.

[25] B. J. McBride, M. J. Zehe, and S. Gordon, "NASA Glenn coefficients for calculating thermodynamic properties of individual species," NASA Technical Report, NASA TP, USA, 2002.